

# 180-degree Outpainting from a Single Image

Zhenqiang Ying<sup>✉</sup>, and Alan C. Bovik, *Fellow, IEEE*

**Abstract**—Presenting context images to a viewer’s peripheral vision is one of the most effective techniques to enhance immersive visual experiences. However, most images only present a narrow view, since the field-of-view (FoV) of standard cameras is small. To overcome this limitation, we propose a deep learning approach that learns to predict a 180-degree panoramic image from a narrow-view image. Specifically, we design a foveated framework that applies different strategies on near-periphery and mid-periphery regions. Two networks are trained separately, and then are employed jointly to sequentially perform narrow-to-90° generation and 90°-to-180° generation. The generated outputs are then fused with their aligned inputs to produce expanded equirectangular images for viewing. Our experimental results show that single-view-to-panoramic image generation using deep learning is both feasible and promising.

**Index Terms**—large field of view, spatially augmented reality, immersion, extrafoveal video

## I. INTRODUCTION

ALTHOUGH image inpainting has been widely studied, its cousin, image outpainting, has been relatively unexplored [1]. Image inpainting algorithms aim to predict relatively small missing or corrupted parts of the interiors of images, based on evidence from surrounding pixels. Ultimately, it may be viewed as a problem of interpolation. By contrast, image outpainting is to extend images beyond their borders, thereby creating larger images with added peripheries. Strictly speaking, this is an extrapolation problem. However, the goal may be to extrapolate a rather large periphery, containing objects and context. Since those two research fields are closely related but slightly different, image inpainting techniques can be borrowed, with some modifications, to repurpose them for image outpainting tasks.

The most common application of image outpainting is to generate context for immersive video extrapolation. By generating peripheral context images to expand the size of an original video content [2], a viewer’s field of view may be greatly expanded, thereby creating a more immersive, vivid, and realistic experience [3]. Although peripheral presentation systems have been constructed [2], [4], [5], [6], they are not yet very popular because of the difficulty of creating the peripheral context images. Here we attack this problem by employing deep neural networks (DNNs). Unlike existing systems that only extend input images horizontally and vertically by a limited extent, we more ambitiously generate 180° panoramic context-images, which if successful, could be used to significantly deepen immersive visual experiences, as exemplified

in Fig. 1. To the best of our knowledge, this is the first such method to be attempted.



Fig. 1. Left: a single-view image. Right: a 180-degree panoramic image generated from the left single-view image.

Single-view-to-panoramic generation is a highly ill-posed inverse problem, since there are infinitely many possible panoramic images that may correspond to a single-view image under essentially any match criterion. One way that we seek to constrain the task is by taking into account properties of peripheral visual perception. First, we exploit the observation that generating high resolution panoramic images is not necessary, since human peripheral vision is lower in spatial resolution than in the central visual field. Because of this, foveated rendering techniques [7], [8] can be used to unlock significant speedups by dividing the image that is to be displayed into multiple sections of varying resolution. Our method uses a foveated framework, both to reduce the computation time and to accelerate network training. In our approach, we allow for a degree of inaccurate or unrealistic image generation in the periphery, because when the image is appropriately viewed, *e.g.*, with a VR device, then the distortions may be designed to be less conspicuous, or even unseen by exploiting the decreased visual acuity in the peripheral visual field [9], as well as visual crowding [10]. Crowding is a phenomenon whereby peripheral vision is not only blurred relative to foveal vision, but may also be perceived as normal even if the peripheral content is otherwise distorted [11], [12], [13]. If properly designed, context images can provide an adequate representation of peripheral vision even if the generated periphery is somewhat distorted.

Just as DNN-based methods have achieved considerable success on solving the image inpainting problem, we build on these concepts, with important modifications, to implement the challenging single-view-to-panoramic image generation task.

We make the following contributions:

- We derive a recommended input field of view and output resolution when generating single-view-to-panoramic images.

The authors are with the Laboratory for Image and Video Engineering Department of Electrical and Computer Engineering, The University of Texas at Austin, Austin, TX 78712 USA.

E-mail: zqying@utexas.edu; bovik@ece.utexas.edu

Manuscript received April XX, 20XX; revised August XX, 20XX.



Fig. 2. Existing peripheral presentation systems. Ambilight TV ©2011, Siberex / <https://commons.wikimedia.org/wiki/File:Ambilight-2.jpg>. AmbiLux TV ©2015, Michael Rathmayr/ <https://mashable.com/2015/09/03/philips-ambilux-projector-tv/>. Other images are from the corresponding papers.

- We design a two-stage foveated framework by which to efficiently spatially extend the image content.
- We use DNNs to generate peripheral image content.
- Because our method does not seek to minimize a boundary error functional, visible boundary effects can occur. To ameliorate this, we deploy a simple blending method to fuse the generated content with the original content along the image boundaries.
- We analyze the experimental results, discuss the limitations of our approach, and consider future work.

## II. RELATED WORK

### A. Peripheral Presentation Systems

Fig. 2 depicts some existing peripheral context generation systems which we can conveniently divide into three categories, each of which we briefly review in the following.

*Image-Plane-Extension Systems.* This concept of peripheral presentation was successfully commercialized to some degree by Philips in the form of the Ambilight TV [14] which uses LED lights on the TV’s rear to throw out colored light that dynamically changes to match the displayed television content. The Philips AmbiLux takes this concept further by using nine pico-projectors on the back of the TV to project an enlarged version of the image [15]. Instead of using multiple projectors, ExtVision [6] displays the peripheral context-images using a single projector mounted on a shelf 6 meters opposite the TV and 2 m above the ground. Those systems mimic a larger screen by extending the visual content horizontally and vertically, but limit the experience to the same plane as the main viewing display [16]. Of course, there is a significant boundary discontinuity between the screen and the periphery.

*Head Mounted Displays.* Although Head-Mounted Displays (HMDs) provide effective immersive experiences for virtual reality, the FoVs of most contemporary systems are still relatively small and do not fill a user’s peripheral field. By adding sparse peripheral displays (SPDs), SparseLightVR [17] and Ambiculus [18] can enlarge the FoV to cover approximately 170 horizontal degrees, while SparseLightVR2 improves the HMD’s FOV to 180 horizontal degrees [19]. The DNN-based

approach of ExtVision [6] was adapted for peripheral context generation in [20].

*CAVE-like systems.* The system called CAVE (cave automatic virtual environment) refers to an immersive virtual reality environment where projectors are directed between three and six walls of a room-sized cube [21]. As compared with affordable and portable HMDs, CAVE-like systems are expensive and require a dedicated, non-portable space. A number of these systems have been developed to approximate CAVE-like systems in the home, such as Infinity-by-nine [22], Surround Video [23], the Microsoft Illumiroom [2] and RoomAlive projects [24], and Razers Project Ariana [25].

### B. Image Completion

Although the terms “image inpainting” and “image completion” are often used interchangeably as well as in isolation, we will use “image completion” to mean the union of the concepts of image inpainting and image outpainting.

*Image Outpainting.* Image outpainting has received much less attention [1] than has image inpainting. Most existing FoV expansion methods are not suitable for this task, since they require additional images of the same environment, e.g. a guide image [28], two supporting images [29], or an online/offline image library [30], [31], [32]. Although generating context images from the image to be extended using patch/block-matching [4], [3], [5] is a straight-forward, albeit very different approach, we advance this process and obtain improved outcomes by applying DNNs trained on substantial amounts of images and context data.

*Image Inpainting.* To fill in small or narrow holes in the image to be viewed, propagating neighborhood appearances based on techniques like the isophote direction field is a simple and effective method [33], [34]. However, these techniques often result in images with significant visual artifacts on large holes. Alternatively, patch-based methods predict missing regions by searching for similar and/or relevant patches from uncorrupted regions of the image [35]. However, a major drawback of these methods lies in the fact that they search for relevant patches based on low-level features over the

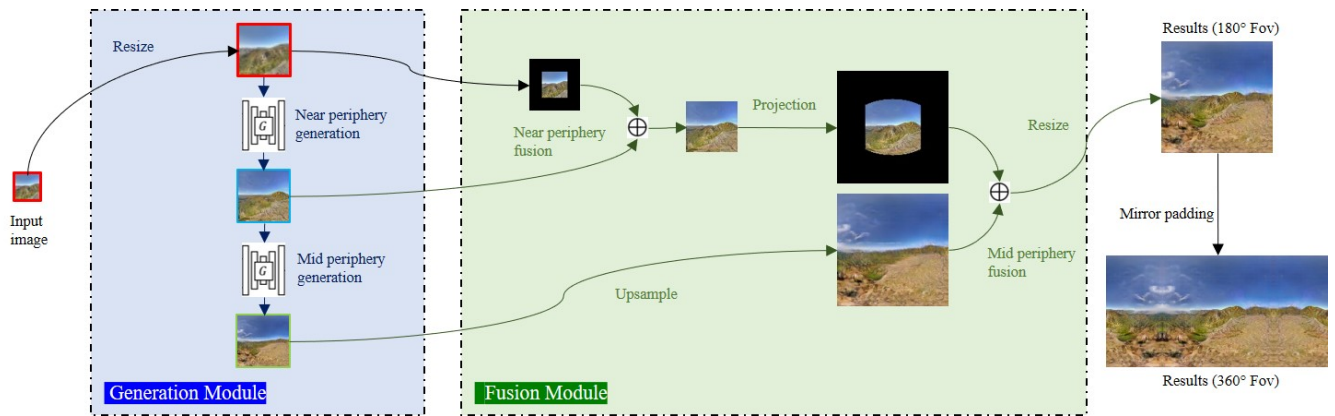


Fig. 3. System pipeline of our panoramic image generator.  $\oplus$  denotes the image fusion operation.

entire image, without using any context or other high-level information to guide the search. Recent years have seen rapid progress in the field of deep image inpainting [36], [37], [38], [27], [39]. However, the classical Context Encoder trained on the outpainting task tends to produce blurry results, as shown in Fig. 4. Moreover, while the state-of-the-art Generative Inpainting method [27] can generate clearer images by “copying” information based on contextual attention, it often produces unrealistic results when copying foreground information to the background. Most inpainting networks are not suitable for the outpainting task, since they assume that the missing contents may be drawn from, or are in some way similar to, parts of the original image. Techniques based on such assumptions, *e.g.* contextual attention, may lead to better inpainting results but worse outpainting outcomes. Finally, techniques that target more challenging inpainting sceneries, such as highly irregular holes [37], further editing [38], or that seek more visually pleasing inpainting results [40], [41], [42], are not necessary in the outpainting setting.

### III. SYSTEM RECOMMENDATIONS

To be able to extend the image content most appropriately and efficiently, we make two system recommendations based on measurements of visual capacity.

#### A. Input FoV Recommendation

Given an image of a fixed resolution, an optimal FoV can be found by finding a best trade-off between image quality and user involvement. As the gaze of a viewer approaches the image center, s/he will feel more involved as the FoV



Fig. 4. Results using existing inpainting networks. Left: Context Encoder [26]; Right: Generative Inpainting [27].

is increased. However, picture flaws arising from a limited resolution become more obvious as the perceived screen size increases. We assume that the input FoV of a single-view-to-panoramic image generation system should be around 50 degrees, which is the optimal FoV based on 1994 guidelines offered by the Society of Motion Picture and Television Engineers (SMPTE) [43].

#### B. Output Resolution Recommendation

Although the human fovea only occupies 1% of the retina, this narrow region is very densely populated with photoreceptors, allowing for high-resolution vision in the vicinity of the point of gaze [6]. By contrast, peripheral vision is much coarser since the density of the photoreceptor decreases rapidly away from the fovea. To model the drop-off of resolution in peripheral vision, we employ the relative spatial frequency function  $r : \Theta \rightarrow [0, 1]$  defined in [44]:

$$r(\theta) = \frac{\beta}{\beta + \theta}, \quad (1)$$

where  $\theta$  is visual angle,  $\Theta$  is the set of viewing angles with respect to the retinal eccentricity, and  $\beta = 2.5^\circ$  is the angle corresponding to the visual angle at which the image becomes only half the resolution of that of the center of gaze ( $\theta = 0^\circ$ ). This function approximates a normal adult’s vision with the exclusion of the blind spot. A higher  $r(\theta)$  indicates higher resolution at visual eccentricity  $\theta$ .

Assume that the viewer’s fixation always falls on the original source image, which implies a maximum visual angle of  $\theta_1$ . The resolution of the input image is assumed to have

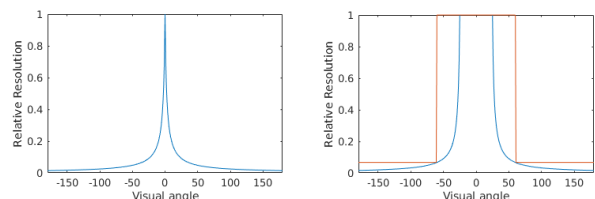


Fig. 5. Left: the relative resolution. Right: the required resolution (in blue) and the system resolution (in red).

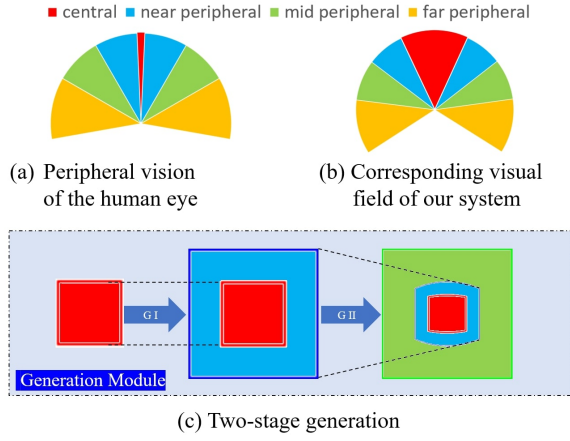


Fig. 6. Two-stage foveated framework.  $G-I$  is the central-to-near-peripheral generator and  $G-II$  is the near-to-mid-peripheral generator.

an uniform, fixed value  $R_1$  over the range of visual angles  $[0, \theta_1]$ . To ensure that the generated peripheral images provide a similar level of visual experience, the resolution at visual angle  $\theta_2$  should be at least

$$R_2 = \frac{r(\theta_2 - \theta_1)}{r(\theta_1 - \theta_1)} R_1 = \frac{\beta}{\beta + \theta_2 - \theta_1} R_1. \quad (2)$$

We plot the recommended relative resolution in Fig. 5 for an optimal visual angle  $25^\circ$  (half of the optimal FoV).

#### IV. SYSTEM IMPLEMENTATION

As shown in Fig. 3, our approach comprises two main processing modules: generation and fusion. First, the input is fed into the generation module, generating two separate outputs that correspond to a  $90^\circ$  FoV and a  $180^\circ$  FoV, respectively. Then, the fusion module fuses the input image with the two outputs to create a panoramic image, which includes the blending process. Finally, the fusion result is mapped to the sphere for viewing. We use the commonly used equirectangular projection as the format for storing panoramic image data.

##### A. Two-stage Foveated Framework

We divide the foveated image generation problem into two stages, as depicted in Fig. 6(c). In the first stage, we extend the image to twice its original size, thereby expanding the FoV to  $90^\circ$ . In the second stage, we further expand the FoV from  $90^\circ$  to  $180^\circ$ . We use two stages rather than one based on two observations:

- The system requires at least two resolution levels, as shown in Fig. 5. This means that if only a low-resolution context image is generated, the viewer will notice the sudden resolution fall-off at the boundary. To alleviate this problem, we can sacrifice a small portion of the original image to form a transition region. Alternatively, if we first outpaint the image to a larger size, then the outpainted region can include the transition region, without reducing the original image. As shown in Fig. 6(b)(c), the final image consists of three regions that roughly correspond, respectively, to the

center ( $0 \sim 50^\circ$  FoV), the near periphery ( $50^\circ \sim 110^\circ$  FoV), and the mid periphery ( $110^\circ \sim 170^\circ$  FoV).

- Although VR devices provide  $360^\circ$  of freedom for viewing, a user can only view  $90^\circ$  at a time on most contemporary devices. On images generated using our framework, a user only sees the generated  $90^\circ$  image when fixating at image center.

Before describing the implementation details, we show that the two-stage framework meets our system requirements. In the first stage, we map the normal FoV to a  $90$ -degree FoV. As shown in Fig. 7,  $ABCD$  is the original image, and we extend the FoV by extending the image both horizontally and vertically, yielding a 4-fold larger image  $A'B'C'D'$ . Given the target FoV  $\alpha'$  of  $90^\circ$ , we have

$$\frac{EF}{E'F'} = \frac{OE}{OE'} = \frac{OP \times \tan(\alpha/2)}{OP \times \tan(\alpha'/2)} = \frac{\tan(\alpha/2)}{\tan(\alpha'/2)}. \quad (3)$$

The input FoV is around  $50^\circ$ , which meets the requirement stated in Sect. III-A:

$$\alpha = 2 \arctan\left(\frac{EF}{E'F'} \tan \frac{\alpha'}{2}\right) = 2 \arctan\left(\frac{1}{2} \tan \frac{90^\circ}{2}\right) \approx 53.13^\circ \quad (4)$$

Regarding the output resolution, the near periphery region has the same resolution as the input, whereas the mid periphery has a lower resolution:

$$R_2 \geq \frac{2.5^\circ}{2.5^\circ + 90^\circ/2 - 53.13^\circ/2} R_1 \approx 0.12 R_1. \quad (5)$$

Following the second stage, the output resolution is about half that of the input, which greatly exceeds our requirements. Therefore, we can resize the image output from stage 2 by a factor of 4 to reduce computation.

##### B. Generation Module

As mentioned earlier, there are two stages in the generation module: near-periphery generation and mid-periphery generation. Both stages can be formulated as an outpainting problem, while the latter one also involves a geometric transformation.

1) *Network Architecture*: We employed pix2pix [45], which has been shown to deliver visually appealing results on the image outpainting problem [6], as our network architecture. Pix2pix has also been used to learn various image-to-image transformation such as “black and white image to color image,” “edge map to natural image,” and “aerial photograph to illustrated map,” and so on. We independently trained two networks, using the pix2pix architecture to learn narrow-to- $90^\circ$  peripheral image generation and  $90^\circ$ -to- $180^\circ$  peripheral

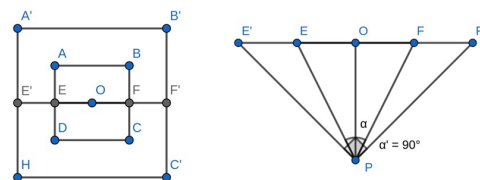


Fig. 7. Calculation of the input FoV of our system.  $O$  is the image center and  $P$  is the location of the viewer.

TABLE I  
PSNR AND NRMSE FOR DIFFERENT GENERATOR ARCHITECTURES.

Category	Criteria	Near periphery generation			Mid periphery generation		
		ResNet_6blocks	ResNet_9blocks	U-Net	ResNet_6blocks	ResNet_9blocks	U-Net
lobby atrium	NRMSE	0.416	0.426	<b>0.373</b>	0.438	0.457	<b>0.417</b>
	PSNR	14.642	14.453	<b>15.609</b>	13.901	13.765	<b>14.524</b>
mountain	NRMSE	0.283	0.280	<b>0.251</b>	0.315	0.329	<b>0.318</b>
	PSNR	16.104	16.325	<b>17.295</b>	<b>15.020</b>	14.581	14.883

image generation. We chose the U-Net [46] as the generator network in pix2pix, since it gives better results as compared with ResNet [47] alternatives, in terms of NRMSE and PSNR between generated images and ground truth images (*c.f.* Table I).

2) *Loss Function*: To produce a visually pleasing outputs, it is necessary to define a suitable loss function. We use the same loss function as was adopted in Pix2pix when training two networks. Pix2pix is a conditional Generative adversarial network(cGAN), optimizing a generator  $G$  by competing with a discriminator  $D$  in a min-max game:

$$G^* = \arg \min_G \max_D \mathcal{L}_{cGAN}(G, D) + \lambda \mathcal{L}_{L1}(G), \quad (6)$$

where  $G$  tries to minimize the loss function against  $D$ , which tries to maximize it. The loss function relatively weights the GAN loss and the L1 loss using the control parameter  $\lambda$ . The GAN loss describes the accuracy of  $D$  in differentiating fake samples  $y^*$  generated by  $G$  and real samples  $y$ :

$$\mathcal{L}_{cGAN}(G, D) = \mathbb{E}_y[\log D(y)] + \mathbb{E}_{y^*}[\log(1 - D(y^*))], \quad (7)$$

while the L1 loss constrains the output to fall close to the ground truth:

$$\mathcal{L}_{L1}(G) = \mathbb{E}_{y, y^*}[\|y - y^*\|_1], \quad (8)$$

where  $\|\cdot\|_1$  is the  $\ell_1$  norm. We also tried the L2 loss in LSGAN [48], but it produces blurry results due to averaging of the possibilities [49]. Using WGAN loss [50] gives sharp results, but it tends to produce artifacts. Therefore, we use the vanilla GAN loss in our method.

### C. Fusion Module

To obtain the final panoramic image, first fuse the input with the generated near periphery image, then fuse the result with the generated mid-periphery image. Before fusing, the images are padded with zeros so they can be aligned on matching domains. We used Poisson blending technique [51] to obtain better fusion results, as shown in Fig. 8.

1) *Divide and Conquer*: While training a single generator to predict the 180° image from the input image would seem to be a straightforward solution, we have found that training two generators to conduct image extrapolation, and 90° to 180° predication, respectively yields better results. In our framework, the final image consists of three parts: the original input image, the generated near peripheral image, and the generated mid peripheral image respectively. This divide and conquer strategy breaks the challenging image generation problem into two parts having different requirements. The near peripheral image requires not only a higher resolution,



Fig. 8. Left: Near periphery fusion with and without blending. Right: Mid periphery fusion with and without blending.



Fig. 9. Halo artifacts when padding the input.

but also less distortion as compared with the mid peripheral image. When fusing the generated peripheral context images with the original images, we noticed that the outputs of the mid periphery generation network yielded relatively poorer continuity with their inputs as compared with those produced by the near periphery generation network. This is probably because the mid-periphery generator conducts both image outpainting as well as geometric transformation. Continuity is much more difficult to preserve while also accounting for geometric inconsistencies between the inputs and outputs. Fortunately, the viewers are unlikely to perceive this discontinuity when fixating at the image center, since 90 degrees of FoV are covered by the generated near-periphery image. The divide and conquer strategy is more efficient than only using outpainting or direct panoramic mapping. If we were to use this network to map the input to 180° directly, the discontinuity would become more obvious and could adversely affect the user experience. It would also be more storage-intensive and time-consuming to generate the 180° image by recursively applying the outpainting network.

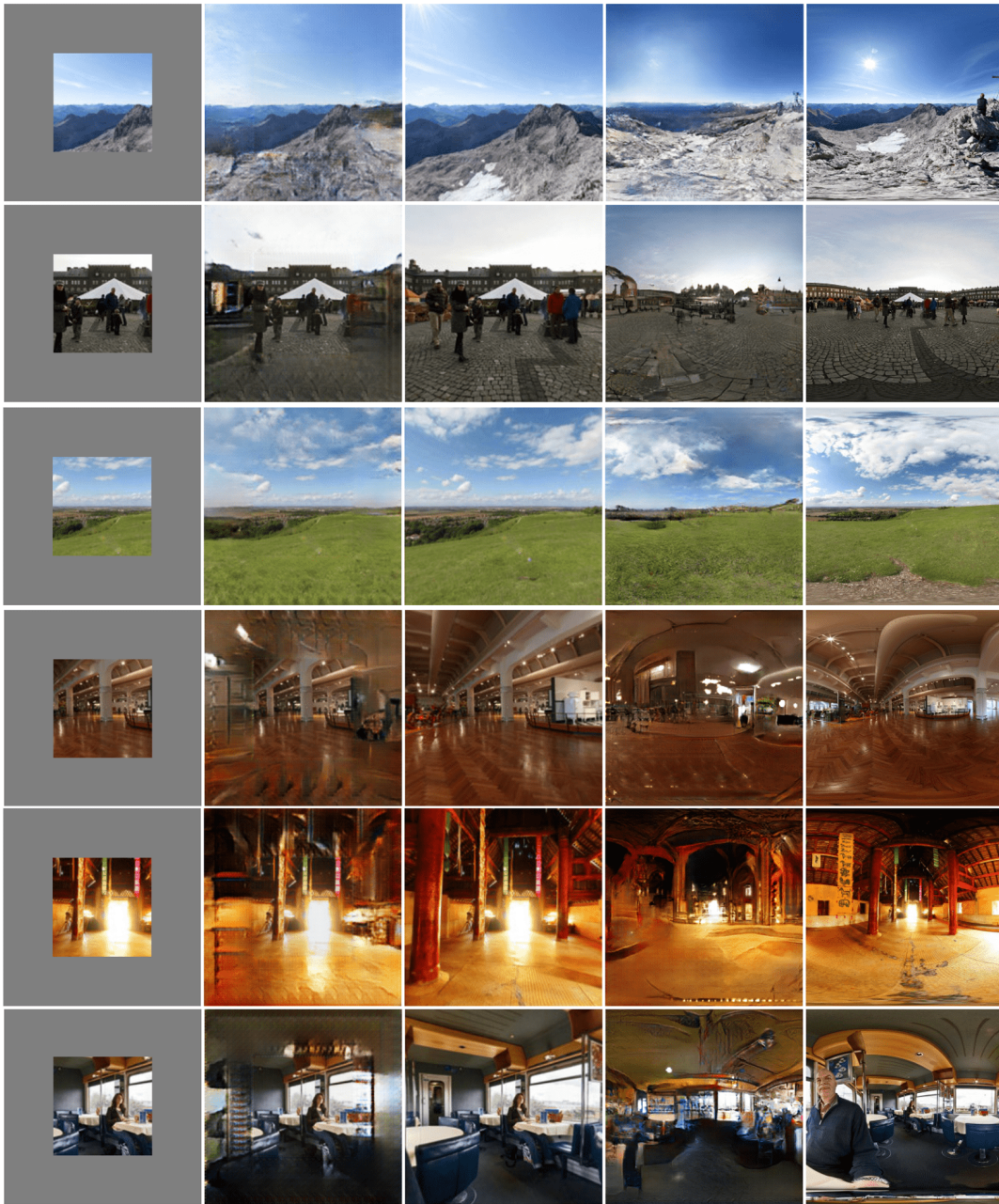


Fig. 10. Single-category results. The networks were trained and tested on three outdoor categories (mountain, street and field) and three indoor categories (lobby atrium, church and restaurant). Each row shows a sample of the held-out images in the validation set of a category. From left to right: the padded input images, the 90° images generated from the inputs, the ground truth 90° images, the 180° images generated from the ground truth 90° images and the ground truth 180° images.

2) *Preprocessing and Postprocessing*: In ExtVision, the input and the output of the generator are aligned by zero-padding the input. As shown in Fig. 9, this may introduce halo artifacts at the image boundaries, since the generator tends to directly copy from the input because of the skip connection of the pix2pix architecture. To avoid direct copying by breaking the alignment, we resize the input instead of zero-padding, leading to better fusion results (see Sect. V).

Since most VR devices only provide 90° of viewing at any moment, a 180° output is adequate provided that the viewer’s fixation lies within the region of the input image. However, outputs having a FoV larger than 180° may be required

in some peripheral presentation systems, since a viewer’s effective FoV can reach 270 degrees with rotation of the eyes and even further with head rotation [3]. In such cases, we can extend the generated 180-degree images to 360 degrees by simply applying a mirror reflected copy operation.

## V. EVALUATION

We trained two generators on image pairs extracted from SUN360 datasets (*c.f.* Sect. V-A). As shown in Fig. 6(c), the first generator produces content for the near periphery (colored in blue) while the second generator produces content for the mid periphery (colored in green). For the second generator, the



Fig. 11. More results on diverse scenes. The first row shows the input images, while the next row shows the outputs generated using our method. Images are from the test set, i.e. the `others` category of the SUN360 dataset. Projection was applied to allow viewing panoramic images in a normal field of view.

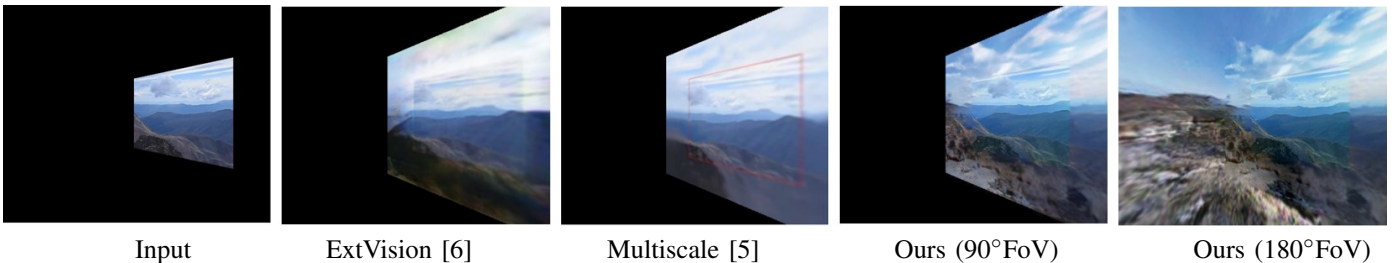


Fig. 12. Comparison with other algorithms. Our method is shown in the far right image. Projection was applied to allow viewing panoramic images in a normal field of view.

input image has a normal field of view while the target image has an equirectangular form. Therefore, geometric translation is involved in addition to image generation.

### A. Datasets

Since most DNN-based methods are data hungry, it is necessary to feed enough data to the networks so that they may learn a sufficiently substantial peripheral representation space. We used the SUN360 dataset [52], which provides diverse panoramic image resolutions up to  $9104 \times 4552$ . For each panoramic image, we selected four input-output pairs: front, back, left, and right. For each direction we generated a pair of images that correspond to an FoV of  $90^\circ$ , and an FoV of  $180^\circ$ , respectively. Those two images were resized to  $256 \times 256$  and fed into the mid periphery generator as input and target, respectively. For the near periphery generator, the  $90^\circ$  image and its central  $1/4$  portion were also resized to  $256 \times 256$  and fed as target and input respectively. The SUN360 dataset provides 14358 indoor images, 52938 outdoor images, and 274 other images. We fused the indoor category with the outdoor category, and held out 100 images for validation. The overall training set contains 268,784 input-output pairs.

### B. Sample Results

The results we obtained using the model trained on images in a specific category are shown in Fig. 10. Results using the model trained on the entire training set of all categories are given in Fig. 11. Since GANs trained on a single category can capture a more accurate distribution as compared with training on images from multiple categories, there is an obvious

performance gap between the single-category results and the multiple-category results. When making comparisons, it is important to remember the exemplars shown on the pages here will appear very different when viewed immersively, especially in the periphery. Nevertheless, the cross-category results are often less acceptable, although very good results are obtained when the categories are similar.

Naturally, it is difficult for a network to generalize well from training data to unseen data. For example, we trained a model only using indoor images, then applied it to the outdoor database. The model tended to draw a ceiling on the top of the rendered output image, since it is very common in the training set. For the central-to-near-peripheral generator, we can use the recursive method [6] to avoid this problem when the input image is from a video. Specifically, we crop the video frames to form original image and cropped image pairs as a training set. However, since all frames have a limited FoV, we could not use this trick for near-to-mid-peripheral generation, which requires a  $180^\circ$  FoV ground truth. Another limitation is the input resolution. Currently, our networks cannot produce context images inputs larger than  $128 \times 128$ , since they only accept a fixed-size input of  $256 \times 256$ . This limitation can be addressed by modifying the network architecture, *e.g.* by adopting fully-convolutional neural networks that can accept images of different resolutions.

### C. Comparison with Existing Systems

We compared against results obtained by two state-of-the-art approaches for image outpainting. Multiscale is PatchMatch-based; while ExtVision is DNN-based.

TABLE II  
AVERAGE IMAGE QUALITY SCORES AMONG SUBJECTS FOR DIFFERENT CATEGORIES AND OUTPAINTING METHODS.

Method	mountain	street	field	lobby_atrium	church	restaurant
ExtVision	68.40	58.90	73.75	52.95	55.45	50.00
ExtVision w/ our blending method	70.65	<b>61.05</b>	78.05	55.15	57.30	54.00
Ours (90°)	<b>77.05</b>	60.35	<b>79.30</b>	<b>65.80</b>	<b>61.80</b>	<b>58.55</b>
AmbiLux TV	72.45	60.25	71.60	53.85	54.20	58.60
Ours (180°)	<b>81.65</b>	<b>61.25</b>	<b>83.20</b>	<b>68.60</b>	<b>65.35</b>	<b>61.85</b>

TABLE III  
PSNR AND NRMSE FOR DIFFERENT CATEGORIES AND OUTPAINTING METHODS (NARROW TO 90° SUB TASK).

Criteria	Model	Indoor categories			Outdoor categories		
		lobby_atrium	church	restaurant	mountain	street	field
NRMSE	ExtVision	0.390	<b>0.397</b>	0.496	0.263	<b>0.369</b>	0.243
	Ours	<b>0.373</b>	0.409	<b>0.435</b>	<b>0.251</b>	0.378	<b>0.237</b>
PSNR	ExtVision	15.183	<b>16.157</b>	13.608	16.642	<b>15.334</b>	17.973
	Ours	<b>15.609</b>	15.947	<b>14.754</b>	<b>17.295</b>	15.214	<b>18.486</b>

TABLE IV  
PSNR AND NRMSE FOR DIFFERENT CATEGORIES AND OUTPAINTING METHODS (90° TO 180° SUB TASK).

Criteria	Model	Indoor categories			Outdoor categories		
		lobby_atrium	church	restaurant	mountain	street	field
NRMSE	AmbiLux	0.437	0.506	0.526	0.332	0.423	0.300
	Ours	<b>0.417</b>	<b>0.459</b>	<b>0.458</b>	<b>0.318</b>	<b>0.398</b>	<b>0.293</b>
PSNR	AmbiLux	13.901	14.353	13.275	14.761	13.561	16.416
	Ours	<b>14.524</b>	<b>15.158</b>	<b>14.505</b>	<b>14.883</b>	<b>14.160</b>	<b>16.577</b>

*Multiscale* [5]. This is a PatchMatch-based video extrapolation method proposed by Aides *et al.*, as an improved version of their earlier work [4]. Both methods use a foveated framework to imitating the resolution variation of the human fovea. The resolution of the extrapolated video diminishes toward the boundaries of the extrapolated region. The process starts at the finest resolution level, *i.e.* the innermost domain, and proceeds outwards from fine to coarse. To improve the scene structure and to better preserve texture, Multiscale instead performs a coarse to fine completion. Although the search for an appropriate patch is limited to within a certain area of the original video to reduce computation time, this approach still requires several minutes to extrapolate one frame, and some artifacts may remain.

*ExtVision* [6]. This work described two methods using a DNN to generate peripheral context-images for videos: a category-limited method and a recursive method. The former uses a network trained on the same category, while the latter uses a network trained on the original video frames. Since we are mainly interested in immersive still images, we use the first method as a comparison. As compared to time-consuming PatchMatch-based approaches, ExtVision ensures a processing speed suitable for real time generation (30 fps). The concurrent work by Sabini *et al.* [1] also treats image outpainting using deep learning algorithms, but only extends the images horizontally.

Fig. 12 shows exemplar results compared to existing methods. ExtVision [6] causes discontinuities to appear at the connection boundaries, because of the direct copy phenomenon mentioned in Sect. IV-C2. Multiscale [5] is a video extrapolation method which requires neighboring frames as inputs. Our

method achieves a more immersive and visual pleasing result, without boundary artifacts and without requiring other frames.

#### D. Human Study

We conducted a human study to investigate the quality of experience (QoE) of panoramic images generated by our method. The generated images were displayed on a HTC Vive VR headset back-ended with a dedicated high performance server (Intel i7-6700, 32GB memory, NVIDIA TITAN X). The interface of the subjective test was built using Unity Game Engine. In the following subsections, we will explain how the images were rated and the detailed protocol of the human study.

1) *Image Quality Scoring*: We recruited 20 students at The University of Texas at Austin, including 7 females and 13 males. Each subject was asked to view a randomized series of panoramic images, and to rate each image with regards to the quality of their viewing experiences, while trying not to be affected by the degree of appeal of the content. We followed the Single Stimulus Continuous Quality evaluation methodology described in recommendation ITU-R BT 500.13 [53] using a continuous rating scale from 0 to 100, where 0 indicates the worst quality.

To limit each subject's viewing time, the quality rating bar appeared after 5 seconds of viewing each image. Five Likert labels (Bad, Poor, Fair, Good, Excellent) marked the rating bar to help guide the subject when making ratings.

2) *Session Design*: Each subject participated in two sessions separated by at least 24 hours, to avoid fatigue. In each session, panoramic images from 6 categories (3 outdoor categories: mountain, street and field; 3 indoor categories:

lobby atrium, church and restaurant) were randomly selected. We randomly picked 3 input images from the test set of each category, and applied different methods to obtain panoramic images for rating. To reduce the effects of visual memory comparisons, images having the same content were separated by at least 3 images of different content.

**Session I: Comparison of 90° outpainting methods.** In this session, the FoV was fixed to 90°. This allowed the subjects to judge the quality of images generated both by ExtVision and by our method. We also implemented and compared ExtVision modified with our blending method to allow for fair comparison only on generated content. Those areas outside of 90° FoV were rendered as black.

**Session II: Comparison of 180° outpainting methods.** Since ExtVision cannot perform 180° outpainting, we could only compare our method against the AmbiLux TV method. To simulate AmbiLux TV, we obtained the 180° panoramic images by resizing the input image.

3) *Results:* The subjective test results are reported in Table II. Our method delivered the highest subjective quality scores among most categories, often by significant margins. We also computed and report the NRMSE and PSNR as references. The quantitative metric results for narrow-to-90° image generation and 90°-to-180° generation are given in Tables III and IV, respectively. Both qualitative and quantitative evaluation show that our method tends to produce more appealing results than existing methods.

We observed that the outpainting task is more challenging on some categories than on others. It is harder to train on a complex, spatially diverse scene (such as the crowded interior of a restaurant) than on a scene containing redundant patterns or textures (such as a field). By comparing the scores reported on two tasks (*c.f.* Tables III and IV), it is apparent that the second task is more challenging. This makes sense, since the second task involves both image outpainting, as well as geometric transformation.

## VI. CONCLUSIONS AND FUTURE WORK

We were able to successfully realize a single-view-to-panoramic image generation system using a deep learning approach. Regarding this challenging task, two system recommendations, a two-stage foveated framework and a DNN-based approach were proposed. While our current approach was created in the context of monoscopic images, the same or similar approaches could be used to enhance immersive stereoscopic images and videos. Our proposed method could also be easily applied to video extrapolation in a frame-by-frame manner, mapping a single-view video to a panoramic video. Since peripheral vision is highly sensitive to flicker [54], a time smoothing filter that averages neighbor frames could be employed to alleviate any flicker problems, as was done in ExtVision [6].

## REFERENCES

[1] Mark Sabini and Gili Rusak, “Painting outside the box: Image outpainting with gans,” *arXiv preprint arXiv:1808.08483*, 2018.

[2] Brett R Jones, Hrvoje Benko, Eyal Ofek, and Andrew D Wilson, “Illumineroom: peripheral projected illusions for interactive experiences,” in *Proceedings of the SIGCHI Conference on Human Factors in Computing Systems*. ACM, 2013, pp. 869–878.

[3] Laura Turban, Fabrice Urban, and Philippe Guillotel, “Extrafoveal video extension for an immersive viewing experience,” *IEEE transactions on visualization and computer graphics*, vol. 23, no. 5, pp. 1520–1533, 2017.

[4] Tamar Avraham and Yoav Y Schechner, “Ultrawide foveated video extrapolation,” *IEEE Journal of Selected Topics in Signal Processing*, vol. 5, no. 2, pp. 321–334, 2011.

[5] Amit Aides, Tamar Avraham, and Yoav Y Schechner, “Multiscale ultrawide foveated video extrapolation,” in *Computational Photography (ICCP), 2011 IEEE International Conference on*. IEEE, 2011, pp. 1–8.

[6] Naoki Kimura and Jun Rekimoto, “Extvision: Augmentation of visual experiences with generation of context images for a peripheral vision using deep neural network,” in *Proceedings of the 2018 CHI Conference on Human Factors in Computing Systems*. ACM, 2018, p. 427.

[7] Anjul Patney, Marco Salvi, Joohwan Kim, Anton Kaplanyan, Chris Wyman, Nir Benty, David Luebke, and Aaron Lefohn, “Towards foveated rendering for gaze-tracked virtual reality,” *ACM Transactions on Graphics (TOG)*, vol. 35, no. 6, pp. 179, 2016.

[8] Brian Guenter, Mark Finch, Steven Drucker, Desney Tan, and John Snyder, “Foveated 3d graphics,” *ACM Transactions on Graphics (TOG)*, vol. 31, no. 6, pp. 164, 2012.

[9] LN Thibos, FE Cheney, and DJ Walsh, “Retinal limits to the detection and resolution of gratings,” *JOSA A*, vol. 4, no. 8, pp. 1524–1529, 1987.

[10] Jerome Y Lettvin, “On seeing sidelong,” *The Sciences*, vol. 16, no. 4, pp. 10–20, 1976.

[11] Ruth Rosenholtz, Jie Huang, and Krista A Ehinger, “Rethinking the role of top-down attention in vision: Effects attributable to a lossy representation in peripheral vision,” *Frontiers in psychology*, vol. 3, pp. 13, 2012.

[12] Lex Fridman, Benedikt Jenik, Shaiyan Keshvari, Bryan Reimer, Christoph Zetsche, and Ruth Rosenholtz, “Sideeye: A generative neural network based simulator of human peripheral vision,” *arXiv preprint arXiv:1706.04568*, 2017.

[13] Lex Fridman, Benedikt Jenik, Shaiyan Keshvari, Bryan Reimer, Christoph Zetsche, and Ruth Rosenholtz, *A Fast Foveated Fully Convolutional Network Model for Human Peripheral Vision*, Verlag nicht ermittelbar, 2017.

[14] A Weffers-Albu, S De Waele, W Hoogenstraaten, and C Kwisthout, “Immersive tv viewing with advanced ambilight,” in *Consumer Electronics (ICCE), 2011 IEEE International Conference on*. IEEE, 2011, pp. 753–754.

[15] “Philips ambilight vs philips ambilux whats the difference?,” <https://www.whathifi.com/promoted/philips-ambilight-vs-philips-ambilux-whats-difference>, Accessed: 2019-01-12.

[16] Daniel Edward Novy, *Computational immersive displays*, Ph.D. thesis, Massachusetts Institute of Technology, 2013.

[17] Robert Xiao and Hrvoje Benko, “Augmenting the field-of-view of head-mounted displays with sparse peripheral displays,” in *Proceedings of the 2016 CHI Conference on Human Factors in Computing Systems*. ACM, 2016, pp. 1221–1232.

[18] Paul Lubos, Gerd Bruder, Oscar Ariza, and Frank Steinicke, “Ambiculus: Led-based low-resolution peripheral display extension for immersive head-mounted displays,” in *Proceedings of the 2016 Virtual Reality International Conference*. ACM, 2016, p. 13.

[19] Abraham M Hashemian, Alexandra Kitson, Thinh Nguyen-Vo, Hrvoje Benko, Wolfgang Stuerzlinger, and Bernhard E Riecke, “Investigating a sparse peripheral display in a head-mounted display for vr locomotion,” in *2018 IEEE Conference on Virtual Reality and 3D User Interfaces (VR)*. IEEE, 2018, pp. 571–572.

[20] Naoki Kimura, Michinari Kono, and Jun Rekimoto, “Using deep-neural-network to extend videos for head-mounted display experiences,” in *Proceedings of the 24th ACM Symposium on Virtual Reality Software and Technology*. ACM, 2018, p. 128.

[21] Carolina Cruz-Neira, Daniel J Sandin, Thomas A DeFanti, Robert V Kenyon, and John C Hart, “The cave: audio visual experience automatic virtual environment,” *Communications of the ACM*, vol. 35, no. 6, pp. 64–73, 1992.

[22] MIT Object Based Media Group, “Infinity-by-nine,” <http://obm.media.mit.edu/>, Accessed: 2019-01-12.

[23] Peter Mills, Alia Sheikh, Graham Thomas, and Paul Debenham, “Surround video,” 2011, p. 5563.

- [24] Brett Jones, Rajinder Sodhi, Michael Murdock, Ravish Mehra, Hrvoje Benko, Andrew Wilson, Eyal Ofek, Blair MacIntyre, Nikunj Raghuvanshi, and Lior Shapira, "Roomalive: magical experiences enabled by scalable, adaptive projector-camera units," in *Proceedings of the 27th annual ACM symposium on User interface software and technology*. ACM, 2014, pp. 637–644.
- [25] Razer, "Project ariana," <http://www.razerzone.com/project-ariana>. Accessed: 2019-01-12.
- [26] Deepak Pathak, Philipp Krahenbuhl, Jeff Donahue, Trevor Darrell, and Alexei A Efros, "Context encoders: Feature learning by inpainting," in *Proceedings of the IEEE Conference on Computer Vision and Pattern Recognition*, 2016, pp. 2536–2544.
- [27] Jiahui Yu, Zhe Lin, Jimei Yang, Xiaohui Shen, Xin Lu, and Thomas S Huang, "Generative image inpainting with contextual attention," *arXiv preprint*, 2018.
- [28] Yinda Zhang, Jianxiong Xiao, James Hays, and Ping Tan, "Framebreak: Dramatic image extrapolation by guided shift-maps," in *Proceedings of the IEEE Conference on Computer Vision and Pattern Recognition*, 2013, pp. 1171–1178.
- [29] Sifeng Xia, Shuai Yang, Jiaying Liu, and Zongming Guo, "Novel self-portrait enhancement via multi-photo fusing," in *Signal and Information Processing Association Annual Summit and Conference (APSIPA), 2016 Asia-Pacific*. IEEE, 2016, pp. 1–4.
- [30] Qi Shan, Brian Curless, Yasutaka Furukawa, Carlos Hernandez, and Steven M Seitz, "Photo uncrop," in *European Conference on Computer Vision*. Springer, 2014, pp. 16–31.
- [31] Juan Leegard Ranteallo Sampetoding, Bagus Satriyawibowo, Rini Wongso, and Ferdinand Ariandy Luwinda, "Automatic field-of-view expansion using deep features and image stitching," *Procedia Computer Science*, vol. 135, pp. 657–662, 2018.
- [32] Miao Wang, Yukun Lai, Yuan Liang, Ralph Robert Martin, and Shi-Min Hu, "Biggerpicture: data-driven image extrapolation using graph matching," *ACM Transactions on Graphics*, vol. 33, no. 6, 2014.
- [33] Michael Ashikhmin, "Synthesizing natural textures.," *SI3D*, vol. 1, pp. 217–226, 2001.
- [34] Coloma Ballester, Marcelo Bertalmio, Vicent Caselles, Guillermo Sapiro, and Joan Verdera, "Filling-in by joint interpolation of vector fields and gray levels," 2000.
- [35] Connelly Barnes, Eli Shechtman, Adam Finkelstein, and Dan B Goldman, "Patchmatch: A randomized correspondence algorithm for structural image editing," in *ACM Transactions on Graphics (ToG)*. ACM, 2009, vol. 28, p. 24.
- [36] Satoshi Iizuka, Edgar Simo-Serra, and Hiroshi Ishikawa, "Globally and locally consistent image completion," *ACM Transactions on Graphics (ToG)*, vol. 36, no. 4, pp. 107, 2017.
- [37] Guilin Liu, Fitsum A Reda, Kevin J Shih, Ting-Chun Wang, Andrew Tao, and Bryan Catanzaro, "Image inpainting for irregular holes using partial convolutions," in *Proceedings of the European Conference on Computer Vision (ECCV)*, 2018, pp. 85–100.
- [38] Jiahui Yu, Zhe Lin, Jimei Yang, Xiaohui Shen, Xin Lu, and Thomas S Huang, "Free-form image inpainting with gated convolution," *arXiv preprint arXiv:1806.03589*, 2018.
- [39] Marcelo Bertalmio, Luminita Vese, Guillermo Sapiro, and Stanley Osher, "Simultaneous structure and texture image inpainting," *IEEE transactions on image processing*, vol. 12, no. 8, pp. 882–889, 2003.
- [40] Chao Yang, Xin Lu, Zhe Lin, Eli Shechtman, Oliver Wang, and Hao Li, "High-resolution image inpainting using multi-scale neural patch synthesis," in *Proceedings of the IEEE Conference on Computer Vision and Pattern Recognition*, 2017, pp. 6721–6729.
- [41] Zhaoyi Yan, Xiaoming Li, Mu Li, Wangmeng Zuo, and Shiguang Shan, "Shift-net: Image inpainting via deep feature rearrangement," in *The European Conference on Computer Vision (ECCV)*, September 2018.
- [42] Wei Xiong, Jiahui Yu, Zhe Lin, Jimei Yang, Xin Lu, Connelly Barnes, and Jiebo Luo, "Foreground-aware image inpainting," in *The IEEE Conference on Computer Vision and Pattern Recognition (CVPR)*, June 2019.
- [43] Ioan Allen, "Screen size: The impact on picture and sound," *SMPTA Journal*, vol. 108, no. 5, pp. 284–289, 1999.
- [44] Ming Jiang, Shengsheng Huang, Juanyong Duan, and Qi Zhao, "Salicon: Saliency in context," in *Proceedings of the IEEE conference on computer vision and pattern recognition*, 2015, pp. 1072–1080.
- [45] Phillip Isola, Jun-Yan Zhu, Tinghui Zhou, and Alexei A Efros, "Image-to-image translation with conditional adversarial networks," in *Proceedings of the IEEE conference on computer vision and pattern recognition*, 2017, pp. 1125–1134.
- [46] Olaf Ronneberger, Philipp Fischer, and Thomas Brox, "U-net: Convolutional networks for biomedical image segmentation," in *International Conference on Medical image computing and computer-assisted intervention*. Springer, 2015, pp. 234–241.
- [47] Kaiming He, Xiangyu Zhang, Shaoqing Ren, and Jian Sun, "Deep residual learning for image recognition," in *Proceedings of the IEEE conference on computer vision and pattern recognition*, 2016, pp. 770–778.
- [48] Xudong Mao, Qing Li, Haoran Xie, Raymond YK Lau, Zhen Wang, and Stephen Paul Smolley, "Least squares generative adversarial networks," in *Proceedings of the IEEE International Conference on Computer Vision*, 2017, pp. 2794–2802.
- [49] Anders Boesen Lindbo Larsen, Søren Kaae Sønderby, Hugo Larochelle, and Ole Winther, "Autoencoding beyond pixels using a learned similarity metric," *arXiv preprint arXiv:1512.09300*, 2015.
- [50] Martin Arjovsky, Soumith Chintala, and Léon Bottou, "Wasserstein gan," *arXiv preprint arXiv:1701.07875*, 2017.
- [51] Patrick Pérez, Michel Gangnet, and Andrew Blake, "Poisson image editing," *ACM Transactions on graphics (TOG)*, vol. 22, no. 3, pp. 313–318, 2003.
- [52] Jianxiong Xiao, Krista A Ehinger, Aude Oliva, and Antonio Torralba, "Recognizing scene viewpoint using panoramic place representation," in *Computer Vision and Pattern Recognition (CVPR), 2012 IEEE Conference on*. IEEE, 2012, pp. 2695–2702.
- [53] BT Series, "Methodology for the subjective assessment of the quality of television pictures," 2012.
- [54] Christopher W Tyler, "Analysis of visual modulation sensitivity. iii. meridional variations in peripheral flicker sensitivity," *JOSA A*, vol. 4, no. 8, pp. 1612–1619, 1987.